

# Roaming dynamics in ion-molecule reactions: phase space reaction pathways and geometrical interpretation

Frédéric A. L. Mauguière\*

*School of Mathematics, University of Bristol,  
Bristol BS8 1TW, United Kingdom*

Peter Collins†

*School of Mathematics, University of Bristol,  
Bristol BS8 1TW, United Kingdom*

Gregory S. Ezra‡

*Department of Chemistry and Chemical Biology, Baker Laboratory,  
Cornell University, Ithaca, NY 14853, United States*

Stavros C. Farantos§

*Institute of Electronic Structure and Laser,  
Foundation for Research and Technology - Hellas, and  
Department of Chemistry, University of Crete, Iraklion 711 10, Crete, Greece*

Stephen Wiggins¶

*School of Mathematics, University of Bristol,  
Bristol BS8 1TW, United Kingdom*

(Dated: November 11, 2018)

## Abstract

A model Hamiltonian for the reaction  $\text{CH}_4^+ \rightarrow \text{CH}_3^+ + \text{H}$ , parametrized to exhibit either early or late inner transition states, is employed to investigate the dynamical characteristics of the roaming mechanism. Tight/loose transition states and conventional/roaming reaction pathways are identified in terms of time-invariant objects in phase space. These are dividing surfaces associated with normally hyperbolic invariant manifolds (NHIMs). For systems with two degrees of freedom NHIMS are unstable periodic orbits which, in conjunction with their stable and unstable manifolds, unambiguously define the (locally) non-recrossing dividing surfaces assumed in statistical theories of reaction rates. By constructing periodic orbit continuation/bifurcation diagrams for two values of the potential function parameter corresponding to late and early transition states, respectively, and using the total energy as another parameter, we dynamically assign different regions of phase space to reactants and products as well as to conventional and roaming reaction pathways. The classical dynamics of the system are investigated by uniformly sampling trajectory initial conditions on the dividing surfaces. Trajectories are classified into four different categories: direct reactive and non reactive trajectories, which lead to the formation of molecular and radical products respectively, and roaming reactive and non reactive orbiting trajectories, which represent alternative pathways to form molecular and radical products. By analysing gap time distributions at several energies we demonstrate that the phase space structure of the roaming region, which is strongly influenced by non-linear resonances between the two degrees of freedom, results in nonexponential (nonstatistical) decay.

PACS numbers: 82.20.-w,82.20.Db,82.20.Pm,82.30.Fi,82.30.Qt,05.45.-a

---

\*Electronic address: frederic.mauguiere@bristol.ac.uk

†Electronic address: peter.collins@bristol.ac.uk

‡Electronic address: gse1@cornell.edu

§Electronic address: farantos@iesl.forth.gr

¶Electronic address: stephen.wiggins@mac.com

## I. INTRODUCTION

New experimental techniques for studying chemical reaction dynamics, such as imaging methods [1] and multidimensional infra-red spectroscopy [2], have revealed unprecedented details of the mechanisms of chemical reactions. The temporal and spatial resolution achieved allows the measurement of reactant and product state distributions, thus providing data that challenge existing theory. Given that accurate quantum dynamical studies can be carried out only for small polyatomic molecules, most theoretical analyses of chemical reaction rates and mechanisms are formulated in terms of classical mechanics (trajectory studies) or statistical approaches, such as RRKM (Rice, Ramsperger, Kassel and Marcus) theory [3, 4] or transition state theory (TST) [5].

A significant challenge to conventional approaches to reaction mechanism is provided by the recently discovered “*roaming reactions*”. This type of reaction was revealed in 2004 by Townsend *et al.* in a study of photodissociation of formaldehyde [6]. When excited by photons, the formaldehyde molecule can dissociate via two channels:  $\text{H}_2\text{CO} \rightarrow \text{H} + \text{HCO}$  (radical channel) or  $\text{H}_2\text{CO} \rightarrow \text{H}_2 + \text{CO}$  (molecular channel). Zee *et al.* [7] found that, above the threshold for the  $\text{H} + \text{HCO}$  dissociation channel, the CO rotational state distribution exhibited an intriguing ‘shoulder’ at lower rotational levels correlated with a hot vibrational distribution of  $\text{H}_2$  co-product. The observed product state distribution did not fit well with the traditional picture of the dissociation of formaldehyde via the well characterized saddle point transition state for the molecular channel. Instead, a new pathway is followed that is dynamical in nature, and such dynamical reaction paths or roaming mechanisms are the central topic of this paper.

The roaming mechanism, which explains the observations of Zee and co-workers, was demonstrated both experimentally and in classical trajectory simulations by Townsend *et al.* [6]. Following this work, roaming has been identified in the unimolecular dissociation of molecules such as  $\text{CH}_3\text{CHO}$ ,  $\text{CH}_3\text{OOH}$  or  $\text{CH}_3\text{CCH}$ , and in ion-molecule reactions [8], and is now recognized as a general phenomenon in unimolecular decomposition (see Ref. [9] and references therein).

Reactions exhibiting roaming pose a considerable challenge to basic understanding concerning the dynamics of molecular reactions. The standard picture in reaction dynamics is firmly based on the concept of the reaction coordinate [10], for example, the *intrinsic reac-*

*tion coordinate* (IRC). The IRC is a minimum energy path (MEP) in configuration space that smoothly connects reactants to products and, according to conventional wisdom, it is the path a system follows (possibly modified by small fluctuations about this path) as reaction occurs. Roaming reactions, instead, avoid the IRC and involve alternative reaction pathways. (It is important to note that reactions involving dynamics that avoids the IRC, so-called non-MEP reactions, were extensively studied before the term “roaming” was coined [11–14].)

For the case of formaldehyde photodissociation, for example, the roaming effect manifests itself by a hydrogen atom nearly dissociating and starting to orbit the HCO fragment at long distances and later returning to abstract the other hydrogen and form the products H<sub>2</sub> and CO. Long-range interactions between dissociating fragments allow the possibility of reorientational dynamics that can result in a different set of products and/or energy distributions than the one expected from MEP intuition, while a dynamical bottleneck prevents facile escape of the orbiting H atom.

The roaming effect has now been identified in a variety of different types of reactions; for example, those involving excited electronic states [15] or isomerization [16, 17]. These studies have identified some general characteristics of the roaming mechanism and point out the need for extending the theories of chemical reactions.

TST is a fundamental approach to calculating chemical reaction rate constants, and can take various forms, such as RRKM theory [3] or variational transition state theory (VTST)[18]. The central ingredient of TST is the concept of a *dividing surface* (DS), which is a surface the system must cross in order to pass from reactants to products (or the reverse). By its very definition, the DS belongs neither to reactants nor to products but is located at the interface between these two species; this is the essence of the notion of *transition state*. Association of transition states with saddle points on the potential energy surface (PES) (and their vicinity) has a long history of successful applications in chemistry, and has provided great insight into reaction dynamics [5, 19, 20]. Accordingly, much effort has been devoted to connecting roaming reaction pathways with the existence (or not) of particular saddle points on the PES, as is evidenced by continued discussion of the role of the so-called “roaming saddle” [21, 22].

It is in fact reasonable to expect that in cases where reactions proceed without a clear correlation to saddles of the PES, they are mediated by transition states that are dynamical

in nature, i.e. *phase space structures*. Phase space formulations of TST have been known since the beginning of the theory [23]. Only in recent years, however, has the phase space (as opposed to a configuration space) formulation of TST reached conceptual and computational maturity [24] for systems with more than two degrees of freedom. Fundamental to this development is the recognition of the role of phase space objects, namely *normally hyperbolic invariant manifolds* (NHIMs) [25], in the construction of relevant DSs for chemical reactions. While the NHIM approach to TST has enabled a deeper understanding of reaction dynamics for systems with many ( $\geq 3$ ) degrees of freedom (DoF) [24, 26], its practical implementation has relied strongly on mathematical techniques to compute NHIMs, such as the normal form theory [27]. Normal form theory, as applied to reaction rate theory, requires the existence of a saddle of index  $\geq 1$  [24] on the PES to construct NHIMs and their attached DSs. For dynamical systems with two DoF the NHIMs are just unstable periodic orbits (PO), which have long been known in this context as Periodic Orbit Dividing Surfaces (PODS). (We recall that a PO is an invariant manifold. In phase space, an unstable PO forms the boundary of the dividing surface for 2 DoF. For natural Hamiltonian systems, kinetic plus potential energy, with 2 DoF, the PODS defines a dividing line in configuration space between reactants and products [28].) As we shall see, these particular hyperbolic invariant phase space structures (unstable POs) are appropriate for describing reaction dynamics in situations where there is no critical point of the potential energy surface in the relevant region of configuration space.

A common characteristic of systems exhibiting roaming reactions studied so far is the presence of long range interactions between the fragments of the dissociating molecule. This characteristic is typical of ion-molecule reactions and roaming is clearly expected to be at play in these reactions. The theory of ion-molecule reactions has a long history going back to Langevin [29], who investigated the interaction between an ion and a neutral molecule in the gas phase and derived an expression for ion-molecule collisional capture rates. As researchers have sought to develop models to account for data on ion-molecule reactions, there has been much debate in the literature concerning the interpretation of experimental results. Some results support a model for reactions taking place via the so-called loose or *orbiting transition states* (OTS), while others rather suggest that the reaction operates through a *tight transition state* (TTS) (for a review, see Ref. 30). In order to explain this puzzling situation the concept of *transition state switching* was developed [30], where both

kinds of TS (TTS and OTS) are present and determine the reaction rate. (See also the unified statistical theory of Miller [31].) Chesnavich presented a simple model to illustrate these ideas [32]. This relatively simple model has all the ingredients required to manifest the roaming effect [33], and the present work extends our investigations of the dynamics of Chesnavich’s model.

In a recent study [33] we have revisited the Chesnavich model [32] in light of recent developments in TST. We have shown that, for barrierless systems such as ion-molecule reactions, the concepts of OTS and TTS can be clearly formulated in terms of well defined phase space geometrical objects (for recent work on the phase space description of OTS, see Ref. 34). We demonstrated how OTS and TTS can be identified with well defined *phase space dividing surfaces* attached to NHIMs. Moreover, this study showed that new reaction pathways, sharing all the characteristics of roaming reactions, may emerge and that they are associated with free rotor periodic orbits, which emanate from *center-saddle bifurcations* (CS).

The Chesnavich model for ion-molecule reactions, parametrised in such a way to represent different classes of molecules with early and late transition states, offers a useful theoretical laboratory for investigation of the evolution of phase space structures relevant to roaming dynamics, both in energy and as a function of additional potential function parameters; such a study is the aim of the present article. The birth of new reaction pathways in phase space associated with non-linear mechanical resonances raises questions concerning the applicability of statistical models. In the present work we investigate these questions with a detailed *gap time analysis* [26, 35, 36] of direct and roaming dynamics.

The paper is organised as follows. In subsection II A we introduce the Hamiltonian of the system to be studied. We then proceed to summarise work on the utility of NHIMs in the context of TST and discuss the DS associated with them in the subsection II B. Subsection II C concludes section II with a discussion of the application of the NHIM approach to the definition of the TTS and OTS in the Chesnavich model. Section III presents a dynamical study of the roaming mechanism. In subsection III A, we provide a discussion of the roaming phenomenon based on an analysis of the dynamics of the Chesnavich model for two different values of the parameter that controls the transition state switching in this model. The role of the so-called “roaming saddle” in the dynamical interpretation of the roaming phenomenon is also discussed. Section IV provides a gap time analysis for the Chesnavich model, while

section V concludes.

## II. HAMILTONIAN, NHIMS AND TRANSITION STATES

### A. System Hamiltonian

More than thirty years ago, the transition state switching model was proposed to account for the competition between multiple transition states in ion-molecule reactions (for a review, see Ref. 30). Multiple transition states were studied by Chesnavich in the reaction  $\text{CH}_4^+ \rightarrow \text{CH}_3^+ + \text{H}$  using a simple model Hamiltonian [32]. The model system consists of two parts: a rigid, symmetric top representing the  $\text{CH}_3^+$  cation, and a mobile H atom. In the following, we employ a simplified version of Chesnavich’s model restricted to two DoF to study roaming.

The Hamiltonian for planar motion with zero overall angular momentum is:

$$H = \frac{p_r^2}{2\mu} + \frac{p_\theta^2}{2} \left( \frac{1}{I_{\text{CH}_3}} + \frac{1}{\mu r^2} \right) + V(r, \theta), \quad (2.1)$$

where  $r$  is the distance between the centre of mass of the  $\text{CH}_3^+$  fragment and the hydrogen atom. The coordinate  $\theta$  describes the relative orientation of the two fragments,  $\text{CH}_3^+$  and H, in a plane. The momenta conjugate to these coordinates are  $p_r$  and  $p_\theta$ , respectively, while  $\mu$  is the reduced mass of the system and  $I_{\text{CH}_3}$  is the moment of inertia of the  $\text{CH}_3^+$  fragment. The potential  $V(r, \theta)$  describes the so-called transitional mode. It is generally assumed that in ion-molecule reactions the different modes of the system separate into intramolecular (or conserved) and intermolecular (or transitional) modes [37–39]. The potential  $V(r, \theta)$  is made up of two terms:

$$V(r, \theta) = V_{\text{CH}}(r) + V_{\text{coup}}(r, \theta), \quad (2.2)$$

with:

$$V_{\text{CH}}(r) = \frac{D_e}{c_1 - 6} \left\{ 2(3 - c_2) \exp [c_1(1 - x)] - (4c_2 - c_1c_2 + c_1)x^{-6} - (c_1 - 6)c_2x^{-4} \right\}, \quad (2.3a)$$

$$V_{\text{coup}}(r, \theta) = \frac{V_0(r)}{2} [1 - \cos(2\theta)], \quad (2.3b)$$

$$V_0(r) = V_e \exp [-\alpha(r - r_e)^2]. \quad (2.3c)$$

Here  $x = r/r_e$ , and parameters fitted to reproduce data from  $\text{CH}_4^+$  species are: dissociation energy  $D_e = 47$  kcal/mol and equilibrium distance  $r_e = 1.1$  Å. Parameters  $c_1 = 7.37$ ,  $c_2 = 1.61$ , fit the polarizability of the H atom and yield a stretch harmonic frequency of



3000  $\text{cm}^{-1}$ . Finally,  $V_e = 55$  kcal/mol is the equilibrium barrier height for internal rotation, chosen so that at  $r = r_e$  the hindered rotor has, in the low energy harmonic oscillator limit, a bending frequency of 1300  $\text{cm}^{-1}$ . The masses are taken to be  $m_H = 1.007825$  u,  $m_C = 12.0$  u, and the moment of inertia  $I_{CH_3} = 2.373409$  u $\text{\AA}^2$ . The parameter  $\alpha$  controls the rate of conversion of the transitional mode from the angular to the radial mode. By adjusting this parameter one can control whether the conversion occurs ‘early’ or ‘late’ along the reaction coordinate  $r$ . For our study we will study the two cases  $\alpha = 1$   $\text{\AA}^{-2}$ , which corresponds to a late conversion, and  $\alpha = 4$   $\text{\AA}^{-2}$ , which corresponds to an early conversion.

Figs 1a and 2a show contour plots of the potential function as well as representative periodic orbits (see section III) for  $\alpha = 1$  and  $\alpha = 4$ , respectively. In Table I, the stationary points of the potential function for the two values of the parameter  $\alpha = 1$  and  $\alpha = 4$  are tabulated and are labelled according to their stability properties. The minimum for  $\text{CH}_4^+$  (EP1) is of center-center (CC) stability type, which means that it is stable in both coordinates,  $r$  and  $\theta$ . The saddle, which separates two symmetric minima at  $\theta = 0$  and  $\pi$  (EP2), is of center-saddle (CS) type, i.e. stable in  $r$  coordinate and unstable in  $\theta$ . The maximum in the PES (EP4) is a saddle-saddle (SS) equilibrium point. The outer saddle (EP3) is a CS equilibrium point.

| $\alpha = 1$          |                      |                |           |       | $\alpha = 4$          |                      |                |           |       |
|-----------------------|----------------------|----------------|-----------|-------|-----------------------|----------------------|----------------|-----------|-------|
| E (kcal mol $^{-1}$ ) | $r$ ( $\text{\AA}$ ) | $\theta$ (rad) | Stability | Label | E (kcal mol $^{-1}$ ) | $r$ ( $\text{\AA}$ ) | $\theta$ (rad) | Stability | Label |
| -47.0                 | 1.1                  | 0              | CC        | EP1   | -47.0                 | 1.1                  | 0              | CC        | EP1   |
| 8.0                   | 1.1                  | $\pi/2$        | CS        | EP2   | 8.0                   | 1.1                  | $\pi/2$        | CS        | EP2   |
| -0.63                 | 3.45                 | $\pi/2$        | CS        | EP3   | -6.44                 | 1.96                 | $\pi/2$        | CS        | EP3   |
| 22.27                 | 1.63                 | $\pi/2$        | SS        | EP4   | 8.82                  | 1.25                 | $\pi/2$        | SS        | EP4   |

TABLE I: Equilibrium points for the potential  $V(r, \theta)$  ( $\alpha = 1$  and 4). (CC) means a center-center equilibrium point (EP), (CS) a center-saddle EP and (SS) a saddle-saddle EP.

The MEP connecting the minimum EP1 with the saddle EP2 at  $r = 1.1$   $\text{\AA}$  (see Figs 1a and 2a) describes a reaction involving ‘isomerisation’ between two symmetric minima. These two isomers cannot of course be distinguished physically for a symmetric Hamiltonian. The MEP for dissociation to radical products ( $\text{CH}_3^+$  cation and H atom) follows the line  $\theta = 0$

with  $r \rightarrow \infty$  and has no potential barrier (or, one might locate the barrier at infinity). Broad similarities between the Chesnavich model and the photodissociation of formaldehyde and other molecules for which the roaming reaction has been observed can readily be identified. In the Chesnavich model we recognize two reaction ‘channels’, one leading to a molecular product by passage through an inner TS, and one to radical products via dissociation. Moreover, a saddle (EP3) exists just below the dissociation threshold, just as has been found in molecules showing the roaming effect.

In the remainder of this article we show that, by adopting a phase space perspective and employing the appropriate transition states defined in phase space, not only is the dynamical meaning of the roaming mechanism revealed but, most importantly, this dynamics is shown to be intimately associated with the generic behavior of non-linear dynamical systems in parameter space, where bifurcations and resonances may occur and qualitatively different dynamics (reaction pathways) are born.

### **B. Transition states, dividing surfaces and statistical assumptions**

TST is based on certain fundamental assumptions [4, 5, 23]. Once these are accepted (or tested for the problem considered), TST provides a powerful and very simple tool for computing the rate constant of a given reaction. One of the assumptions is the existence of a DS having the property that classical trajectories originating in reactants (resp. products) cross this surface only once in proceeding to products (resp. reactants). Such a DS therefore separates the phase space into two distinct regions, reactants and products, and therefore constitutes the boundary between them. The definition of the DS given above is fundamentally dynamical in nature (the local non-recrossing condition). The DS is in general a surface in the phase space of the system under consideration. Computing, or locating, a phase space surface (hypersurface/volume) that realises the first assumption of TST is in general not an easy task as one has to find a codimension one hypersurface in a  $2n$ -dimensional space for an  $n$  DoF system. As discussed below, the NHIM approach to TST provides a solution to this problem.

A comment on nomenclature: The term ‘transition state’ is sometimes used to designate a saddle point of the system potential energy surface. Identification of the *transition state* with a point in configuration space is of course misleading; a transition state is more precisely

defined as the manifold of phase space points where the transition between reactants and products occurs. The phase space DS defined above is just such a collection of phase space transition points. Confusion between saddle points and TS (DS) arises in situations where the system has to overcome a barrier in the PES in order to react. In such a case, there is a saddle point (index one) at the top of the barrier and the DS (TS) originates (in phase space) in the vicinity of this saddle point. However, there are situations for which the reaction does not proceed via a potential barrier and in these cases one has to find other phase space structures that define DS (TS). We have seen that the Chesnavich model provides an example where the outer TS is not associated with any potential saddle.

In searching for the appropriate DS for which the (local) non-recrossing property applies, and thus the minimal reactive flux criterion, it is reasonable to start with stationary points on the PES. However, minimization of the flux by varying the DS in configuration space as in variational transition state theory (VTST)[18] may give a better DS. In this approach, the DS is still defined in configuration space but its location along some reaction path is determined by a variational principle. One can also investigate the flux through surfaces of specified geometry to determine optimal dividing surfaces in a given family of such surfaces (for an example of such a surface applied to the roaming phenomenon see Ref. 39).

The minimal flux through the DS requirement can be cast into a minimum of the sum of states at the DS. As we move along some reaction coordinate from reactants to products, there is two competing effects which affect the sum of states in the DS [31]. First, as we move to the dissociation products the potential energy is constantly rising and the available kinetic energy is decreasing which has the effect of lowering the sum of states. The second effect is a lowering of the vibrational frequencies at the DS that tends to increase the sum of states. These two competing effects result in a minimum in the sum of states located at some value of the reaction coordinate. This minimum has been called an “entropic barrier” for the reaction or a tight transition state. On the other hand, in the orbiting model of a complex forming the DS is located at the centrifugal barrier induced by the effective potential (the orbiting TS) [30, 31]. In general the TTS and OTS are not located at the same position along the reaction coordinate and so one can ask which of these two DS should be used to compute the rate of the reaction. This problem gives rise to the theory of multiple transition states where one has to decide which DS (TTS or OTS) to use in the computation of the rate of the reaction. The Chesnavich model provides an excellent example [30, 32, 40]. In this

model both TS (DS) exist simultaneously and the actual TS (DS) for the computation of the reaction rate in a naive TST calculation is the one giving the minimal flux or, equivalently, the minimal sum of states. Millers’s approach provides a unified theory appropriate when the fluxes associated with each DS are of comparable magnitude. We will see in the next paragraph how the Chesnavich model is treated within the NHIM approach to TST and in the next section how this approach relates to the roaming phenomenon.

The other fundamental assumption of TST is that of statistical dynamics. If one considers the reaction at a specific energy, the statistical assumption requires that throughout the dissociation of the molecule all phase space points are equally probable on the timescale of reaction [4]. This assumption is equivalent to saying that the redistribution of the energy amongst the different DoF of the system on the reactant side of the DS is fast compared to the rate of the reaction, and guarantees a single exponential decay for the reaction (random lifetime assumption for the reactant part of the phase space [35]). In section IV we will investigate this statistical assumption for the roaming phenomenon by studying the gap time distributions in the “roaming region” defined in section III.

### C. Normally hyperbolic invariant manifolds and their related dividing surfaces

In this section we summarise recent work which has shown the usefulness of NHIMs in the context of TST [24]. In the previous subsection we recalled that TST is build on the assumption of the existence of a DS separating the phase space into two parts, reactant and products. The construction of this surface has been the subject of many studies. As we emphasized, the DS is in general a surface in phase space, and the construction of such surfaces for systems with three and higher DoF has until recently been a major obstacle in the development of the theory.

For systems with two DoF described by a natural Hamiltonian, kinetic plus potential energy, the construction of the DS is relatively straightforward. This problem was solved during the 1970s by McLafferty, Pechukas and Pollak [41–44]. They showed that the DS at a specific energy is intimately related to an invariant phase space object, an unstable PO. The PO defines the bottleneck in phase space through which the reaction occurs and the DS which intersects trajectories evolving from reactants to products can be shown to have the topology of a hemisphere whose boundary is the PO [45, 46]. The same construction

can be carried out for a DS intersecting trajectories travelling from products to reactants and these two hemispheres form a sphere for which the PO is the equator.

Generalisation of the above construction to higher dimensional systems has been a major question in TST and has only received a satisfactory answer relatively recently [45, 46]. The key difficulty concerns the higher dimensional analogue of the unstable PO used in the two DoF problem for the construction of the DS. Results from dynamical systems theory show that transport in phase space is controlled by various high dimensional manifolds, Normally Hyperbolic Invariant Manifolds (NHIMs), which are the natural generalisation of the unstable PO of the two DoF case. Normal hyperbolicity of these invariant manifolds means that they are, in a precise sense, structurally stable, and possess stable and unstable invariant manifolds that govern the transport in phase space [25, 47–49].

Existence theorems for NHIMs are well established [25, 47–49], but for concrete examples one needs methods to compute them. One approach involves a procedure based on Poincaré-Birkhoff normalisation: the idea is to find a set of canonical coordinates by means of canonical transformations that put the Hamiltonian of the system in a “simple” form in a neighbourhood of an equilibrium point of saddle-centre...-centre type (an equilibrium point at which the linearized vector field has one pair of real eigenvalues and  $n - 1$  imaginary eigenvalues for a system of  $n$  DoF). The “simplicity” comes from the fact that, under non-resonance conditions among the imaginary frequencies at the saddle point, one can construct an integrable system valid in the neighbourhood of the equilibrium point and thereby describe the dynamics in this neighbourhood very simply. With this new Hamiltonian, the geometrical structures that govern reaction dynamics are revealed. For two DoF systems, the NHIM is simply a PO. For an  $n > 2$  DoF system at a fixed energy, the NHIM has the topology of a  $(2n - 3)$  sphere. This  $(2n - 3)$ -dimensional sphere is the equator of a  $(2n - 2)$ -dimensional sphere which constitutes the DS. The DS divides the  $(2n - 1)$ -dimensional energy surface into two parts, reactants and products, and one can show that it is a surface of *minimal flux* [45].

The NHIM approach to TST consists of constructing DSs for the reaction studied built from NHIMs, and constitutes a rigorous realisation of the local non-recrossing property. Once these geometrical objects (NHIM and DS) are computed the reactive flux from reactant to products through the DS can easily be expressed as the integral of a flux form over the DS. Furthermore, it is possible to sample the DS and use this knowledge to propagate classical

trajectories initiated at the TS (DS). As noted above, for the two DoF case, the unstable PO used in the construction of the DS is just an example of such a NHIM. In this paper, we are concerned with an  $n = 2$  DoF problem and therefore the NHIMs we will be interested in are POs. Extension to  $n > 2$  DoF systems is in principle conceptually straightforward.

### III. ROAMING DYNAMICS

#### A. Dynamical interpretation of the roaming mechanism

In the previous section, we discussed the notions of TTS and OTS in the context of a reaction occurring without a potential barrier. We also discussed how the NHIM approach to TST provides a rigorous way of constructing a DS that satisfies the local no-recrossing requirement of TST. To define DSs that are relevant for the description of reactions in the model Hamiltonian defined in Eq. (2.1), we need to locate unstable POs. Periodic orbits for conservative Hamiltonian systems exist in *families*, where the POs in a family depend on system parameters. In molecular systems, for example, it is very common to consider PO families obtained by variation of the energy of the system (see for example Refs. 50 and 51). At critical parameter values (the energy, for example) bifurcations take place and new families are born. Continuation/bifurcation (CB) diagrams are obtained by plotting a PO property as a function of the parameter. One important kind of elementary bifurcation is the center-saddle, which turns out to be ubiquitous in non-linear dynamical systems [27]. Although periodic orbits, being one dimensional objects, cannot reveal the full structure of phase space, they do provide a “skeleton” around which more complex structures such as invariant tori develop. Numerous explorations of non-linear dynamical systems by construction of PO CB diagrams have been made. In particular, for molecules with multidimensional, highly anharmonic and coupled potential functions, software has been developed to locate POs based on multiple shooting algorithms [52], and has successfully been applied to realistic models of small polyatomic molecules [50]. In Figs. 1b and 2b such CB diagrams are shown for the Chesnavich model for the values of the parameter  $\alpha = 1$  and  $\alpha = 4$  respectively. Not all principal families of POs generated from all equilibria are shown, but only those which are relevant for our discussion of the roaming phenomenon.

We identify the DS constructed from the PO denoted TTS-PO in Figs. 1b and 2b with the TTS. These periodic orbits show hindered rotor behavior. The OTS is related to the centrifugal barrier appearing due to the presence of the centrifugal ( $\approx r^{-2}$ ) term in the kinetic energy, Eq. (2.1). There is in fact a PO associated with the centrifugal barrier, referred to as a *relative equilibrium*. In Figs. 1b and 2b we refer to this PO as OTS-PO and we identify the DS constructed from this PO with the OTS. These relative equilibrium POs

and higher dimensional analogues have been studied by Wiesenfeld et al. [34] in the context of capture theories of reaction rates.

We have therefore clearly identified the notions of TTS and OTS found in the literature with DSs constructed from NHIMs. These TSs (DSs) are surfaces which satisfy rigorously the requirement of local no-recrossing TST theory. These two TSs (DSs) exist simultaneously for our model Hamiltonian and in the following we discuss the dynamical consequences of this fact and how one can interpret roaming phenomenon in this setting.

### 1. *Roaming and non-linear mechanical resonances*

The TTS and OTS are associated with different reactive bottlenecks in the system, and hence, in a certain sense, with different ‘reaction pathways’. In order to completely dissociate to  $\text{CH}_3^+ + \text{H}$ , the system has to cross the OTS. This surface satisfies a global non-recrossing condition (as opposed to a local non-recrossing condition) in the sense that once the system crosses this surface in the outward sense the orbital momentum is an approximate constant of motion (for sufficiently large  $r$ ), and the system enters an uncoupled free rotor regime. The TTS, on the other hand, is the DS associated with formation of the cation  $\text{CH}_4^+$ . These two DS delimit an intermediate region defining the association complex  $\text{CH}_3^+ \cdots \text{H}$ . The picture here is similar to that discussed by Miller in his Unified Statistical Theory [31], where a modified statistical theory is developed to describe association/dissociation dynamics in the presence of a complex. In Miller’s theory, the complex was associated with a well in the PES, whereas in our case, there is actually no potential well in the intermediate region between the TTS and OTS with which the complex can be unambiguously associated. Instead, there are non-linear mechanical resonances, which create ‘sticky’ regions in phase space (for rigorous results on the notion of stickiness in Hamiltonian systems see [53, 54]). These resonances are marked by the families of periodic orbits FR1 and its period doublings (for example FR12), so that the phase space region delimited by the TTS and the OTS can be thought of as a “dynamical complex”.

The two TTS and OTS form two phase space bottlenecks between which trajectories can be trapped for arbitrary long times. This trapping is responsible for the existence of trajectories for which the hydrogen atom winds around the  $\text{CH}_3^+$  fragment and “roams” before exiting the dynamical complex, either to reform  $\text{CH}_4^+$  or to dissociate to  $\text{CH}_3^+ + \text{H}$ . Hence, the



dynamical complex defines the *roaming region*. To study this trapping phenomenon we initiate classical trajectories on the OTS and follow them either until the  $\text{CH}_4^+$  cation is formed or dissociation back to  $\text{CH}_3^+ + \text{H}$  occurs. Trajectory propagation is then stopped shortly after crossing of the TTS or OTS occurs. We make such calculations for two different values of the parameter  $\alpha$  which controls the location of the TS in the Chesnavich transition state switching model. In the next paragraph we describe these classical trajectory simulations.

## 2. Classical trajectory simulations

To perform our classical trajectory simulation we uniformly sample trajectory initial conditions on the OTS at constant energy (microcanonical sampling). As explained in section II, the OTS-DS is composed of two parts: one hemisphere for which the trajectories cross from reactants to products (forward hemisphere) and the other for which the trajectories cross from products to reactants (backward hemisphere). For the OTS, if we define as reactants the complex  $\text{CH}_3^+ \cdots \text{H}$  and as products  $\text{CH}_3^+ + \text{H}$ , in our simulation we are interested only in trajectories lying on the backward hemisphere of the DS. We sample this hemisphere uniformly and numerically integrated the equations of motion until the trajectories cross either the OTS (forward hemisphere this time) or the TTS (backward hemisphere if  $\text{CH}_4^+$  is defined as reactants and the complex  $\text{CH}_3^+ \cdots \text{H}$  as the products for the TTS).

We wish to classify trajectories according to qualitatively different types of behavior, i.e., trajectories associated with different reactive events. Two obvious qualitatively different types of trajectories can be identified. First, there are trajectories which cross the TTS and form  $\text{CH}_4^+$ . These trajectories are ‘reactive’ trajectories. Second, there are trajectories which recross the OTS to form  $\text{CH}_3^+ + \text{H}$ . These trajectories are ‘non reactive’.

Our classification scheme requires a precise definition of ‘roaming’ trajectories. In a previous publication [33] we proposed a classification of trajectories according to the number of turning points in the  $r$  coordinate. Here, in light of subsequent investigations involving gap times (see the next section), we refine this definition of roaming. In the present system, roaming is intuitively associated with motions in which the hydrogen atom orbits the  $\text{CH}_3^+$  fragment while undergoing oscillations in the  $r$  coordinate. For such motions to occur, energy must be transferred from the radial to the angular mode and (see below) the mechanism for such an energy transfer involves non-linear resonances, which are manifest by the appearance

of the FR1 POs. Just as we construct DS associated with the TTS-POs and the OTS-POs, it is possible to define a DS associated with the FR1 PO, which we denote the FR1-DS. To exhibit roaming character according to our revised definition, a trajectory must cross the FR1-DS several times. Such a trajectory will therefore involve exchange of energy between the radial and angular DoF before finding its way to a final state (either  $\text{CH}_4^+$  or  $\text{CH}_3^+ + \text{H}$ ).

We now define the four categories of trajectories used in our analysis of the Chesnavich model:

- Direct reactive trajectories: these trajectories cross the FR1-DS only once before crossing the TTS to form  $\text{CH}_4^+$ .
- Roaming reactive trajectories: these trajectories cross the FR1-DS at least three times before crossing the TTS to form  $\text{CH}_4^+$ . Note that a reactive trajectory has to cross the FR1-DS an odd number of times.
- Direct non reactive trajectories: these trajectories cross the FR1-DS only twice before crossing the OTS to form  $\text{CH}_3^+ + \text{H}$ .
- Roaming non reactive trajectories: these trajectories cross the FR1-DS at least four times before crossing the OTS to form  $\text{CH}_3^+ + \text{H}$ . Note non reactive trajectories have to cross the FR1-DS an even number of times.

Note that, in principle there may be non reactive trajectories which never cross the FR1-DS but which return immediately to recross the OTS. The existence of these trajectories is perfectly conceivable as the stable and unstable manifolds of the period doubling bifurcated orbits of the FR1 family, could ‘reflect back’ the incoming trajectories. However, we find no such trajectories in our simulations.

Trajectories were propagated and classified into the four different classes according to the definitions given above for two different values of the parameter  $\alpha$  of the Hamiltonian. In the Chesnavich model, this parameter controls the “switching” of the transition state from late to early. The switching model was developed in the context of variational TST where it is necessary to determine the optimal transition state to use in a statistical theory in order to compute the reaction rate. A variational criterion is used to select the relevant TS, tight or loose. In the system under study here, two phase space DS (TTS and OTS) exist simultaneously, and in order to analyze the roaming phenomenon in dynamical terms,

both must be taken into account. In the next section, we investigate the question of the assumption of statistical dynamics in the roaming region.

In Fig. 3 we show the result of our classical trajectory simulations at energy  $E = 0.5$  kcal/mol for the case  $\alpha = 1$ . The case  $\alpha = 1$  corresponds to the switching occurring late, which means that if one were to use variational TST an OTS would be used to compute the rate. In Fig. 3 the TTS-PO, the FR1 and the OTS-PO are represented as thick black curves. Each panel of the figure shows trajectories belonging to different classes of trajectories that we defined earlier. Fig. 3a shows the direct reactive trajectories, Fig. 3b the roaming reactive trajectories, Fig. 3c the direct non reactive trajectories and Fig. 3d the roaming non reactive trajectories. Similarly, Fig. 4 shows the results for the case  $\alpha = 4$  at the same energy.

Figure 5 shows the evolution of the TTS-PO with  $\alpha$  at constant energy of  $0.5 \text{ kcal.mol}^{-1}$ . The location of the OTS remains practically unchanged with  $\alpha$ . In order to quantify the roaming effect we plot in Fig. 6 the fractions of the different classes of trajectories versus energy. Fig. 6a is for the case  $\alpha = 1$  and Fig. 6b for  $\alpha = 4$ . It is also instructive to look at the rotor angular momentum ( $p_\theta$ ) distributions for the direct and roaming non reactive trajectories at the beginning and the end of the trajectory propagation. The angular momentum distributions for direct trajectories and those exhibiting roaming are found to be qualitatively different in experiments [6] and Figs. 7 and 8 show that our classification scheme captures this aspect of the roaming phenomenon for our model system. Fig. 7 shows initial and final angular momentum distributions for the case  $\alpha = 1$  at several energies and similarly Fig. 8 for the case  $\alpha = 4$ . Both initial and final distributions are identical within the statistical errors, as is expected since the OTS PO defines the only entrance (exit) portal for the association (dissociation) of radical reactants (products) to occur.

There has been an interesting discussion in the literature concerning the possible existence of a saddle in the PES responsible for the roaming reaction, often referred to as the “the roaming saddle” [21, 39, 55, 56]. Indeed, for the Chesnavich model, there exists such a saddle point on the PES, labelled EP3 in Table I, which could be considered to be a roaming saddle. However, as has already been pointed out, transition states are in general not associated with particular potential saddles. We have shown that the TTS and OTS are the dividing surfaces associated with unstable periodic orbits, those of TTS-PO and OTS-PO families, which originate from center-saddle bifurcations (see Figs. 1b and 2b). On the other hand, equilibria of the PES, both stable and unstable, are essential in tracing the birth of time

invariant objects in phase space, such as principal families of periodic orbits, tori, NHIMs and other invariant manifolds.

The existence of ubiquitous center–saddle bifurcations of periodic orbits is supported by the Newhouse theorem [27, 57], which was initially proved for dissipative dynamical systems, and later extended to Hamiltonian systems [58, 59]. The theorem states that tangencies of the stable and unstable manifolds associated with unstable equilibria and periodic orbits generate an infinite number of period doubling and center–saddle bifurcations. Hence, the unstable periodic orbits of the principal family of EP3 (Lyapunov POs) are expected to generate such CS bifurcations as their manifolds extend along the bend degree of freedom. Intersections of these manifolds, either self-intersections or with manifolds from different equilibria, generate homoclinic and heteroclinic orbits, respectively [27]. Such orbits can connect remote regions of phase space. This phenomenon has been repeatedly underlined in explorations of the phase space of a variety of small polyatomic molecules [50, 51, 60]. The numerical location of such bi-asymptotic orbits is not easy, and this fact makes periodic orbit families even more precious in studying the complexity of the molecular phase space at high excitation energies.

The FR1 POs are associated with a 2:1 resonance region in phase space between stretch ( $r$ ) and bend ( $\theta$ ) modes. The CS bifurcation generates “out of nowhere” stable and unstable PO branches. In this way we can understand the trapping of (non) reactive trajectories in the roaming mechanism, and can also assign a DS attached to the NHIM FR1-PO.

## IV. GAP TIME ANALYSIS OF THE ROAMING REGION

In the preceding section, we described the dynamics of roaming reactions. We showed that the TTS and the OTS delimit a roaming region inside which some trajectories may be trapped for long times, and that roaming region can be seen as a dynamical complex even if there is no well in the PES with which this complex can be associated. The situation is very similar to that described in Miller’s unified treatment of statistical theory in the presence of a complex [31]. Our analysis showed that the roaming region can be viewed as a dynamical complex, and it is therefore relevant to investigate the validity of the assumption of statistical dynamics within the roaming region.

To investigate the nature of dynamics in the roaming region, we perform a gap time analysis. We will first briefly review the gap time approach to reaction rates due to Thiele [35, 36]. Our exposition follows closely Ref. 26 to which we refer the reader for more information.

Many theoretical investigations have been made of the validity of the statistical assumption underlying TST, focusing on the lifetime and gap time distributions of species involved. A non exhaustive list of important work includes the reserarch of Slater [61, 62], Bunker [63, 64], Bunker and Hase [65], Thiele [35, 36], Dumont and Brumer [66] and DeLeon and co-workers [67, 68]. Broadly speaking, nonstatistical or non-RRKM behavior for a specific unimolecular dissociation reaction can arise in two essentially different ways. First, for a specific reaction, non-RRKM behavior can be observed because reactants are prepared in a specific state which violates the assumption of uniform phase space density in the reactant region. The second possible origin of non-RRKM behavior is due to inherent non-statistical intramolecular dynamics, so-called intrinsic non-RRKM behavior [65].

### A. Gap time approach to unimolecular reaction rates

#### 1. Phase space volumes, gap times and microcanonical RRKM rates

To introduce the essential concepts needed, we will first treat the case for which the reactant is described by a single well to which access is mediated by a single channel (DS). (For this case, cf. Fig. 1 of Ref. 26.) As noted previously, for a given energy, a DS constructed from NHIMs divides the energy surface into two distinct species, reactants and products. Furthermore, the DS is composed of two hemispheres, one of which intersects trajectories

travelling from reactant to product, and controls exit from the well, the other of which intersects trajectories travelling from products to reactants, and controls the access to the well. The hemisphere which controls the access to the well is designated  $DS_{in}(E)$  and that which controls the exit from the well  $DS_{out}(E)$ , where the (microcanonical) DS is defined at constant energy  $E$ . The distinct phase space regions corresponding to reactants and products are denoted  $\mathcal{M}_r$  and  $\mathcal{M}_p$ , respectively. The microcanonical density of states for reactant species is:

$$\rho_r(E) = \int_{\mathcal{M}_r} d\mathbf{x} \delta(E - H(\mathbf{x})), \quad (4.1)$$

where  $\mathbf{x} \in \mathbb{R}^{2n}$  designate a phase space point for an  $n$  DoF system. A similar expression can be written for the product part of the phase space  $\mathcal{M}_p$ . The points on the reactant part of the phase space can be uniquely specified by coordinates  $(\bar{q}, \bar{p}, \psi)$ , where  $(\bar{q}, \bar{p}) \in DS_{in}(E)$  is a point on  $DS_{in}(E)$  specified by  $2(n-1)$  coordinates  $(\bar{q}, \bar{p})$ , and  $\psi$  is a time variable. The point  $\mathbf{x}(\bar{q}, \bar{p}, \psi)$  is reached by propagating the initial condition  $(\bar{q}, \bar{p}) \in DS_{in}(E)$  forward for time  $\psi$ . As all initial conditions on  $DS_{in}(E)$  will leave the reactant region in finite time by crossing  $DS_{out}(E)$ , for each  $(\bar{q}, \bar{p}) \in DS_{in}(E)$  we can define the *gap time*  $s = s(\bar{q}, \bar{p})$ , which is the time it takes for the incoming trajectory to traverse the reactant region. That is,  $\mathbf{x}(\bar{q}, \bar{p}, \psi = s(\bar{q}, \bar{p})) \in DS_{out}(E)$ . For the phase point  $\mathbf{x}(\bar{q}, \bar{p}, \psi)$ , we therefore have  $0 \leq \psi \leq s(\bar{q}, \bar{p})$ .

The coordinate transformation  $\mathbf{x} \rightarrow (E, \psi, \bar{q}, \bar{p})$  is canonical [35, 69, 70] so that the phase space volume element is

$$d^{2n}\mathbf{x} = dE d\psi d\sigma, \quad (4.2)$$

with  $d\sigma \equiv d^{n-1}\bar{q} d^{n-1}\bar{p}$  an element of  $2n-2$  dimensional area on the DS. We denote the flux across  $DS_{in}(E)$  and  $DS_{out}(E)$  by  $\phi_{in}(E)$  and  $\phi_{out}(E)$ , respectively, and note that  $\phi_{in}(E) + \phi_{out}(E) = 0$ . For our purposes we only need the magnitude of the flux, and so set  $|\phi_{in}(E)| = |\phi_{out}(E)| \equiv \phi(E)$  the magnitude  $\phi(E)$  of the flux through dividing surface  $DS_{in}(E)$  at energy  $E$  is given by

$$\phi(E) = \left| \int_{DS_{in}(E)} d\sigma \right|, \quad (4.3)$$

where the element of area  $d\sigma$  is precisely the restriction to  $DS_{in}(E)$  of the appropriate flux  $(2n-2)$ -form,  $\omega^{n-1}/(n-1)!$ , corresponding to the Hamiltonian vector field associated with  $H(\mathbf{x})$ . The reactant phase space volume occupied by points initiated on the dividing surface

$DS_{in}(E)$  with energies between  $E$  and  $E + dE$  is therefore

$$dE \int_{DS_{in}(E)} d\sigma \int_0^s d\psi = dE \int_{DS_{in}(E)} d\sigma s = dE \phi(E) \bar{s}, \quad (4.4)$$

where the *mean gap time*  $\bar{s}$  is defined as

$$\bar{s} = \frac{1}{\phi(E)} \int_{DS_{in}(E)} d\sigma s. \quad (4.5)$$

From this we conclude that the reactant density of state associated with trajectories that enter and exit the well region is

$$\rho_r^c(E) = \phi(E) \bar{s}, \quad (4.6)$$

where the superscript  $c$  denotes that this density refers to *crossing* trajectories (some trajectories may be trapped in the well region and never escape from it). Equation 4.6 is the content of the so-called spectral theorem [69, 71–74]. If all phase space points in the reactant region  $\mathcal{M}_r$  were to react, we would have  $\rho_r^c(E) = \rho_r(E)$ , where  $\rho_r(E)$  now denotes the density of states for the full reactant region  $\mathcal{M}_r$ . However, because of the existence of trapped trajectories, in general we have  $\rho_r^c(E) \leq \rho_r(E)$ . If  $\rho_r^c(E) < \rho_r(E)$  it is then necessary to introduce corrections to the statistical estimate of the reaction rate [68, 75–79].

The statistical (RRKM) microcanonical rate for the forward reaction from reactant to products at energy  $E$  is given by

$$k_{RRKM}(E) = \frac{\phi(E)}{\rho_r(E)}, \quad (4.7)$$

and if  $\rho_r^c(E) = \rho_r(E)$ , we then have

$$k_{RRKM}(E) = \frac{1}{\bar{s}}. \quad (4.8)$$

In general the inverse of the mean gap time is given by

$$\frac{1}{\bar{s}} = \frac{\phi(E)}{\rho_r^c(E)} = k_{RRKM}(E) \left[ \frac{\rho_r(E)}{\rho_r^c(E)} \right] \equiv k_{RRKM}^c(E) \geq k_{RRKM}(E), \quad (4.9)$$

where the superscript in  $k_{RRKM}^c(E)$  is for corrected *RRKM* microcanonical rate.

Generalisation to situations for which the access/exit to the reactant region is controlled by  $d$  DSs gives for the corrected RRKM rate (see Ref. [26])

$$k_{RRKM}^c(E) = \frac{\sum_{i=1}^d \phi_i(E)}{\sum_{i=1}^d \bar{s}_{DS_{i,in}(E)} \phi_i(E)} \quad (4.10)$$

## 2. Gap time and lifetime distributions

An important notion in the gap time formulation of TST is the gap time distribution,  $P(s; E)$ : the probability that a phase space point on  $DS_{in}(E)$  at energy  $E$  has a gap time between  $s$  and  $s + ds$  is equal to  $P(s; E) ds$ . The statistical assumption of TST is equivalent to the requirement that the gap time distribution is the random, exponential distribution

$$P(s; E) = k(E) \exp(-k(E)s). \quad (4.11)$$

This distribution is characterised by a single exponential decay constant  $k(E)$  function of the energy to which corresponds the mean gap time  $\bar{s}(E) = k(E)^{-1}$ .

The lifetime of a phase space point  $\mathbf{x}(\bar{q}, \bar{p}, \psi)$  is the time needed for this point to exit the reactant region  $\mathcal{M}_r$  by crossing  $DS_{out}(E)$  and is then defined as  $t = s(\bar{q}, \bar{p}) - \psi$ . It can be shown (see Ref. [26]) that the lifetime distribution function  $\mathbb{P}(t; E)$  is related to the gap time distribution by

$$\mathbb{P}(t; E) = \frac{1}{\bar{s}} \int_t^{+\infty} ds P(s; E). \quad (4.12)$$

An exponential gap time distribution (satisfying the statistical assumption) implies that the lifetime distribution is also exponential.

Finally, in addition to the gap time distribution itself, we also consider the integrated gap time distribution  $F(t; E)$ , which is defined as the fraction of trajectories on the DS with gap times  $s \geq t$ , and is simply the product of the normalized reactant lifetime distribution function  $\mathbb{P}(t; E)$  and the mean gap time  $\bar{s}$

$$F(t; E) = \bar{s} \mathbb{P}(t; E) = \int_t^{+\infty} ds P(s; E). \quad (4.13)$$

For the random gap time distribution the integrated gap time distribution is exponential,  $F(t; E) = \exp(-kt)$ .

### B. Trajectory simulations of gap time distributions

In order to test the statistical assumption for the roaming region we analyze the gap time distributions for this phase space region. To do so, we sample the OTS microcanonically on the incoming hemisphere and integrate trajectories initiated at these sample points until they recross either the OTS or the TTS.



Gap time distributions obtained from these simulations are shown in Figs. 9 and 10 for  $\alpha = 1$  and  $\alpha = 4$ , respectively. Each of these figures has 4 panels, corresponding to different energies. In each panel we show the normalised gap time distributions for each of the four classes of trajectories we defined earlier, as well as the gap time distribution for all the trajectories taken together. Details are given in the captions of the figures.

The integrated gap time distributions for the same samples used in Figs 9 and 10 are shown in Figs 11 and 12, respectively. As seen in these figures, the gap time distributions, as well as the integrated gap time distributions, exhibit significant deviation from random (exponential) distributions, indicating that the statistical dynamical assumption of TST is not satisfied for motion in the roaming region.

In Fig 13 we plot the sampled trajectory initial conditions on the OTS in the  $(\theta, p_\theta)$  plane; different colors are used to represent trajectory initial conditions belonging to different classes. This plot reveals a succession of *bands* of different types on the DS (see, for example, ref. 80 and references therein). The arrangement of bands can be very complicated (fractal) [81]. In Fig 14 we plot gap time versus  $p_\theta$  for initial conditions on the OTS at fixed  $\theta = 0$  for a range of  $p_\theta$  values. The plot shows the fractal nature of bands associated with different trajectory types, and indicates that gap times diverge at the boundary between bands associated with two different trajectory types [42, 82]. An infinitely fine sampling of the  $p_\theta$  axis would presumably reveal a set of measure zero of initial conditions for which the gap times are infinite. Infinite gap times correspond to trajectories trapped forever in the roaming regions, and such trajectories are on the stable invariant manifolds of stationary objects in the roaming region, such as the FR1 PO and its period doubling bifurcations.

## V. SUMMARY AND CONCLUSION

The model Hamiltonian for the reaction  $\text{CH}_4^+ \rightarrow \text{CH}_3^+ + \text{H}$  proposed by Chesnavich [32] to study transition state switching in ion-molecule reactions has been employed to investigate roaming dynamics. The Chesnavich model supports multiple transition states and, despite its simplicity, is endowed with all the essential characteristics of systems previously found to exhibit the roaming mechanism.

Using concepts and methods from non-linear mechanics, early/late or tight/loose transition states are identified with time invariant objects in phase space, which are dividing surfaces in phase space associated with NHIMs – normally hyperbolic invariant manifolds. For two degree of freedom systems NHIMs are unstable periodic orbits which define the boundaries of locally non-recrossing dividing surfaces assumed in statistical reaction rate theories such as TST. The roaming region of phase space is itself unambiguously defined by these dividing surfaces.

By constructing continuation/bifurcation diagrams of periodic orbits for two values of the parameter in the Chesnavich Hamiltonian model controlling the early versus late nature of the transition state, and using the total energy as a second parameter, we identify phase space regions associated with roaming reaction pathways (i.e., trapping in the roaming region). The classical dynamics of the system are investigated by microcanonically sampling the outer OTS DS and assigning trajectories to four different classes: direct reactive and direct non-reactive, which describe the formation of molecular and radical products respectively, and roaming reactive and roaming non reactive, which follow alternative pathways to formation of molecular and radical products.

We identify the TTS and OTS with dividing surfaces associated with unstable periodic orbits of the TTS-PO and OTS-PO families. Additional PO families such as the FR1 POs reveal alternative reaction pathways, the roaming pathway, and define region in phase space associated with a 2:1 resonance between the stretch ( $r$ ) and the bend ( $\theta$ ) modes. The CS bifurcations generate “out of nowhere” a branch with stable and a branch with unstable periodic orbits. In this way we can understand the dynamical origin of the trapping of (non) reactive trajectories in the roaming region.

To investigate the validity of the assumption of statistical dynamics for the microcanonical ensembles we consider, we have analysed gap time distributions at several energies. Lifetime

distributions exhibit multiple exponential dissociation rates at long times, violating the assumption of random gap times underlying statistical theory.

By plotting the outcome for trajectory initial conditions initiated on the  $(\theta, p_\theta)$  at the OTS DS, we observe a regular succession of ‘bands’ of different types of trajectories. Our numerical results indicate the existence of a fractal band structure, where the gap time diverges at the boundary between distinct trajectory types. Such divergent gap times are associated with initial conditions on the stable manifold of invariant objects in the roaming region such as the FR1 PO and its period doubling bifurcations.

It is worth emphasizing that the concepts, theory and algorithms described here for two degrees of freedom systems can in principle be straightforwardly extended to higher dimensional systems. Nevertheless, substantial technical difficulties need to be overcome for accurate computation of NHIM-DS for higher dimensional systems.

### **Acknowledgments**

This work is supported by the National Science Foundation under Grant No. CHE-1223754 (to GSE). FM, PC, and SW acknowledge the support of the Office of Naval Research (Grant No. N00014-01-1-0769), the Leverhulme Trust, and the Engineering and Physical Sciences Research Council (Grant No. EP/K000489/1).

- 
- [1] M. N. R. Ashfold, N. Nahler, A. Orr-Ewing, O. Vieuxmaire, R. Toomes, T. Kitsopoulos, I. Garcia, D. Chestakov, S. Wu, and D. Parker, *Phys. Chem. Chem. Phys.* **8**, 26 (2006).
- [2] S. Mukamel, *Ann. Rev. Phys. Chem.* **51**, 691 (2000).
- [3] W. Forst, *Unimolecular Reactions* (Cambridge University Press, Cambridge, 2003).
- [4] T. Baer and W. L. Hase, *Unimolecular Reaction Dynamics* (Oxford University Press, New York, 1996).
- [5] R. D. Levine, *Molecular Reaction Dynamics* (Cambridge University Press, 2009).
- [6] D. Townsend, S. A. Lahankar, S. K. Lee, S. D. Chambreau, A. G. Suits, X. Zhang, J. Rheinecker, L. B. Harding, and J. M. Bowman, *Science* **306**(5699), 1158 (2004).
- [7] R. D. van Zee, M. F. Foltz, and C. B. Moore, *J. Chem. Phys.* **99**(3), 1664 (1993), URL <http://link.aip.org/link/?JCP/99/1664/1>.
- [8] H. G. Yu, *Phys. Scr.* **84**, 028104 (2011).
- [9] J. M. Bowman and B. C. Shepler, *Ann. Rev. Phys. Chem.* **62**, 531 (2011).
- [10] D. Heidrich, ed., *The Reaction Path in Chemistry: Current Approaches and Perspectives* (Springer, New York, 1995).
- [11] L. P. Sun, K. Y. Song, and W. L. Hase, *Science* **296**, 875 (2002).
- [12] J. G. Lopez, G. Vayner, U. Lourderaj, S. V. Addepalli, S. Kato, W. A. Dejong, T. L. Windus, and W. L. Hase, *J. Am. Chem. Soc.* **129**, 9976 (2007).
- [13] J. Mikosch, S. Trippel, C. Eichhorn, R. Otto, U. Lourderaj, J. X. Zhang, W. L. Hase, M. Weidemüller, and R. Wester, *Science* **319**, 183 (2008).
- [14] J. Zhang, J. Mikosch, S. Trippel, R. Otto, M. Weidemüller, R. Wester, and W. L. Hase, *J. Phys. Chem. Lett.* **1**(18), 2747 (2010).
- [15] M. P. Grubb, M. L. Warter, H. Xiao, S. Maeda, K. Morokuma, and S. W. North, *Science* **335**, 1075 (2012).
- [16] I. G. Ulusoy, J. F. Stanton, and R. Hernandez, *J. Phys. Chem. A* **117**, 7553 (2013).
- [17] I. G. Ulusoy, J. F. Stanton, and R. Hernandez, *J. Phys. Chem. A* **117**, 10567 (2013).
- [18] D. G. Truhlar and B. C. Garrett, *Ann. Rev. Phys. Chem.* **35**, 159 (1984).
- [19] B. K. Carpenter, *Determination of Organic Reaction Mechanisms* (Wiley, New York, 1984).
- [20] D. J. Wales, *Energy Landscapes* (Cambridge University Press, Cambridge, 2003).

- [21] B. C. Shepler, Y. Han, and J. M. Bowman, *J. Phys. Chem. Lett.* **2**(7), 834 (2011).
- [22] L. B. Harding, S. J. Klippenstein, and A. W. Jasper, *J. Phys. Chem. A* **116**, 6967 (2012).
- [23] E. P. Wigner, *Trans. Faraday Soc.* **34**, 29 (1938).
- [24] H. Waalkens, R. Schubert, and S. Wiggins, *Nonlinearity* **21**, R1 (2008).
- [25] S. Wiggins, *Normally hyperbolic invariant manifolds in dynamical systems* (Springer-Verlag, New York, 1994).
- [26] G. S. Ezra, H. Waalkens, and S. Wiggins, *J. Chem. Phys.* **130**, 164118 (2009).
- [27] S. Wiggins, *Introduction to Applied Nonlinear Dynamical Systems and Chaos* (Springer-Verlag, New York, 2003), second ed.
- [28] P. Pechukas, *Ann. Rev. Phys. Chem.* **32**, 159 (1981).
- [29] P. Langevin, *Annal. Chim. Phys.* **5**, 245 (1905).
- [30] W. J. Chesnavich and M. T. Bowers, *Theory of Ion-Neutral Interactions: Application of Transition State Theory Concepts to Both Collisional and Reactive Properties of Simple Systems* (Pergamon Press, 1982).
- [31] W. H. Miller, *J. Chem. Phys.* **65**, 2216 (1976).
- [32] W. J. Chesnavich, *J. Chem. Phys.* **84**, 2615 (1986).
- [33] F. A. L. Mauguire, P. Collins, G. S. Ezra, S. C. Farantos, and S. Wiggins, *Chem. Phys. Lett.* **592**, 282-27 (2014).
- [34] L. Wiesenfeld, *Adv. Chem. Phys.* **130 A**, 217 (2005).
- [35] E. Thiele, *J. Chem. Phys.* **36**(6), 1466 (1962).
- [36] E. Thiele, *J. Chem. Phys.* **38**(8), 1959 (1963).
- [37] S. R. Vande Linde and W. L. Hase, *J. Phys. Chem.* **94**(16), 6148 (1990).
- [38] G. H. Peslherbe, H. Wang, and W. L. Hase, *J. Chem. Phys.* **102**(14), 5626 (1995), URL <http://scitation.aip.org/content/aip/journal/jcp/102/14/10.1063/1.469294>.
- [39] S. J. Klippenstein, Y. Georgievskii, and L. B. Harding, *J. Phys. Chem. A* **115**, 14370 (2011).
- [40] W. J. Chesnavich, L. Bass, T. Su, and M. T. Bowers, *J. Chem. Phys.* **74**(4), 2228 (1981).
- [41] P. Pechukas and F. J. McLafferty, *J. Chem. Phys.* **58**(4), 1622 (1973), URL <http://scitation.aip.org/content/aip/journal/jcp/58/4/10.1063/1.1679404>.
- [42] P. Pechukas and E. Pollak, *J. Chem. Phys.* **67**(12), 5976 (1977), URL <http://scitation.aip.org/content/aip/journal/jcp/67/12/10.1063/1.434777>.
- [43] E. Pollak and P. Pechukas, *J. Chem. Phys.* **69**, 1218 (1978).

- [44] P. Pechukas and E. Pollak, *J. Chem. Phys.* **71**(5), 2062 (1979), URL <http://scitation.aip.org/content/aip/journal/jcp/71/5/10.1063/1.438575>.
- [45] H. Waalkens and S. Wiggins, *J. Phys. A: Math. Gen.* **37**(35), L435 (2004).
- [46] S. Wiggins, L. Wiesenfeld, C. Jaffé, T. Uzer, *et al.*, *Phys. Rev. Lett.* **86**(24), 5478 (2001).
- [47] N. Fenichel, *Indiana Univ. Math. J.* **21**(193-226), 1972 (1971).
- [48] N. Fenichel, *Indiana Univ. Math. J.* **26**, 81 (1977), ISSN 0022-2518.
- [49] N. Fenichel, *Indiana Univ. Math. J.* **23**, 1109 (1974), ISSN 0022-2518.
- [50] S. C. Farantos, R. Schinke, H. Guo, and M. Joyeux, *Chem. Rev.* **109**(9), 4248 (2009).
- [51] F. Mauguere, M. Rey, V. Tyuterev, J. Suarez, and S. C. Farantos, *J. Phys. Chem. A* **114**(36), 9836 (2010).
- [52] S. C. Farantos, *Comput. Phys. Commun.* **108**, 240 (1998).
- [53] A. D. Perry and S. Wiggins, *Physica D* **71**(1-2), 102 (1994).
- [54] A. Morbidelli and A. Giorgilli, *J. Stat. Phys.* **78**(5-6), 1607 (1995).
- [55] L. B. Harding, S. J. Klippenstein, and A. W. Jasper, *Phys. Chem. Chem. Phys.* **9**, 4055 (2007).
- [56] L. B. Harding and S. J. Klippenstein, *J. Phys. Chem. Lett.* **1**(20), 3016 (2010).
- [57] S. E. Newhouse, *Publ. Math. IHES* **50**, 101 (1979).
- [58] P. Duarte, *Dyn. Stab. Sys.* **14**(4), 339 (1999).
- [59] S. V. Gonchenko and L. P. Silnikov, *J. Stat. Phys.* **101**(1/2), 321 (2000).
- [60] F. A. L. Mauguere, S. C. Farantos, J. Suarez, and R. Schinke, *J. Chem. Phys.* **134**(24), 244302 (2011).
- [61] N. B. Slater, *J. Chem. Phys.* **24**(6), 1256 (1956).
- [62] N. B. Slater, *Theory of Unimolecular Reactions* (Cornell University Press, Ithaca, NY, 1959).
- [63] D. L. Bunker, *J. Chem. Phys.* **37**, 393 (1962).
- [64] D. L. Bunker, *J. Chem. Phys.* **40**, 1946 (1964).
- [65] D. L. Bunker and W. L. Hase, *J. Chem. Phys.* **59**, 4621 (1973).
- [66] R. S. Dumont and P. Brumer, *J. Phys. Chem.* **90**, 3509 (1986).
- [67] N. DeLeon and B. J. Berne, *J. Chem. Phys.* **75**, 3495 (1981).
- [68] B. J. Berne, N. DeLeon, and R. O. Rosenberg, *J. Phys. Chem.* **86**, 2166 (1982).
- [69] J. Binney, O. E. Gerhard, and P. Hut, *Mon. Not. Roy. Astron. Soc.* **215**, 59 (1985).
- [70] H.-D. Meyer, *J. Chem. Phys.* **84**, 3147 (1986).
- [71] P. Brumer, D. E. Fitz, and D. Wardlaw, *J. Chem. Phys.* **72**(1), 386 (1980).

- [72] E. Pollak, J. Chem. Phys. **74**, 6763 (1981).
- [73] H. Waalkens, A. Burbanks, and S. Wiggins, Phys. Rev. Lett. **95**, Art. No. 084301 (2005).
- [74] H. Waalkens, A. Burbanks, and S. Wiggins, J. Phys. A **38**, L759 (2005).
- [75] W. L. Hase, D. G. Buckowski, and K. N. Swamy, J. Phys. Chem. **87**, 2754 (1983).
- [76] S. Y. Grebenshchikov, R. Schinke, and W. L. Hase, in *Unimolecular Kinetics: Part 1. The Reaction Step*, edited by N. J. B. Greene (Elsevier, New York, 2003), vol. 39 of *Comprehensive Chemical Kinetics*, pp. 105–242.
- [77] M. Berblinger and C. Schlier, J. Chem. Phys. **101**, 4750 (1994).
- [78] S. K. Gray and S. A. Rice, J. Chem. Phys. **86**, 2020 (1987).
- [79] J. N. Stember and G. S. Ezra, Chem. Phys. **337**, 11 (2007).
- [80] Y. Nagahata, H. Teramoto, C. Li, S. Kawai, and T. Komatsuzaki, Phys. Rev. E **88**, 042923 (2013).
- [81] M. Grice, B. Andrews, and W. Chesnavich, J. Chem. Phys. **87**, 959 (1987).
- [82] F. Mauguere, P. Collins, G. Ezra, and S. Wiggins, J. Chem. Phys. **138**, 134118 (2013).

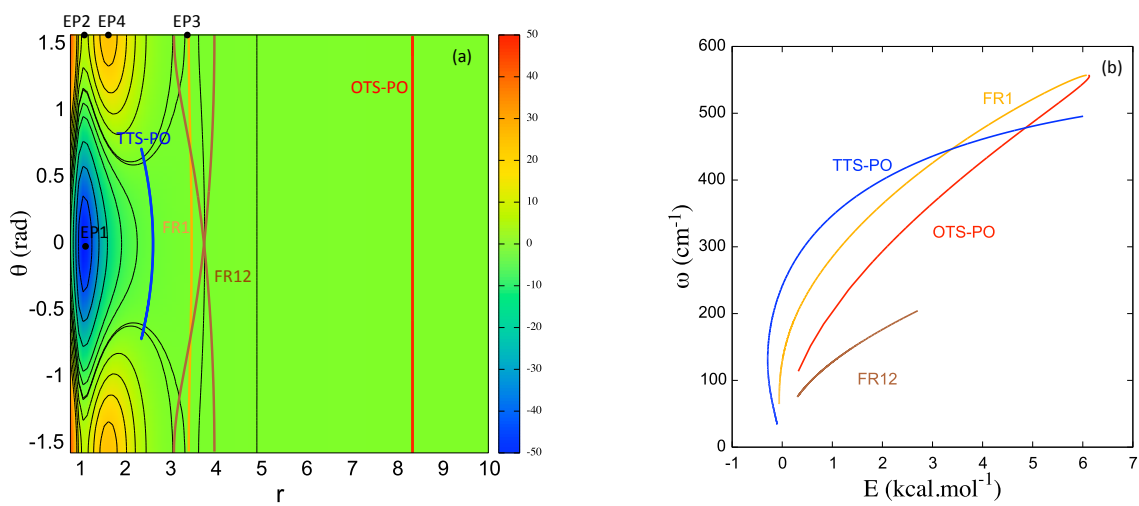


FIG. 1: (a) Contour plot of the PES for  $\alpha = 1$  with representative POs. (b) Continuation/bifurcation diagram of families of periodic orbits for  $\alpha = 1$ .



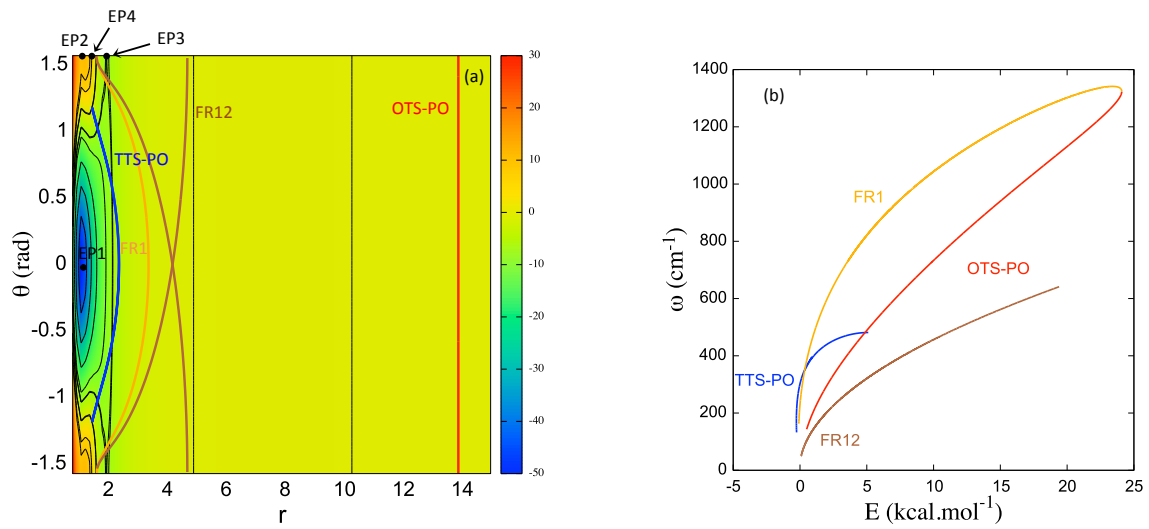


FIG. 2: (a) Contour plot of the PES for  $\alpha = 4$  with representative POs. (b) Continuation/bifurcation diagram of families of periodic orbits for  $\alpha = 4$ .

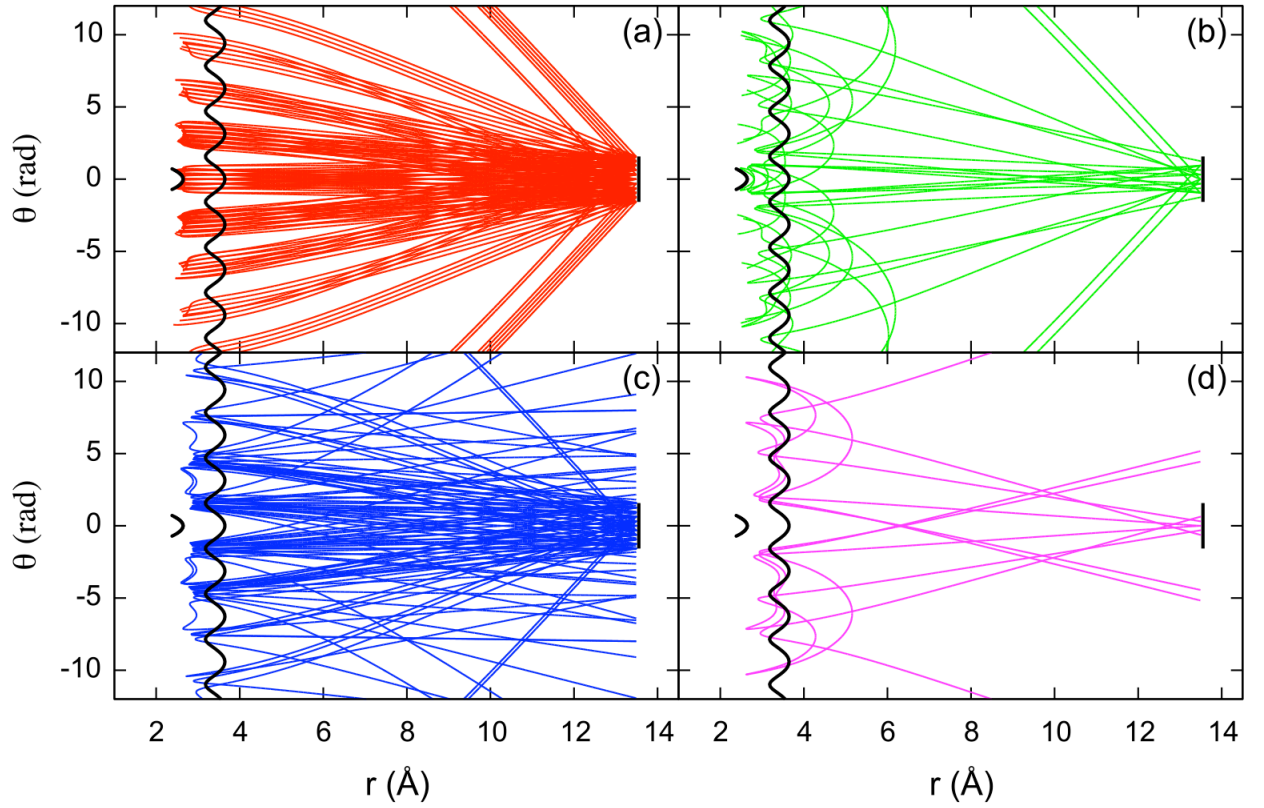


FIG. 3: The four different types of trajectories for the case  $\alpha = 1$ . The thick black curves correspond to the TTS-PO, FR1 PO and OTS PO, respectively. (a) direct reactive trajectories (red). (b) Roaming reactive trajectories (green). (c) Direct non reactive trajectories (blue). (d) Roaming non reactive trajectories (magenta).

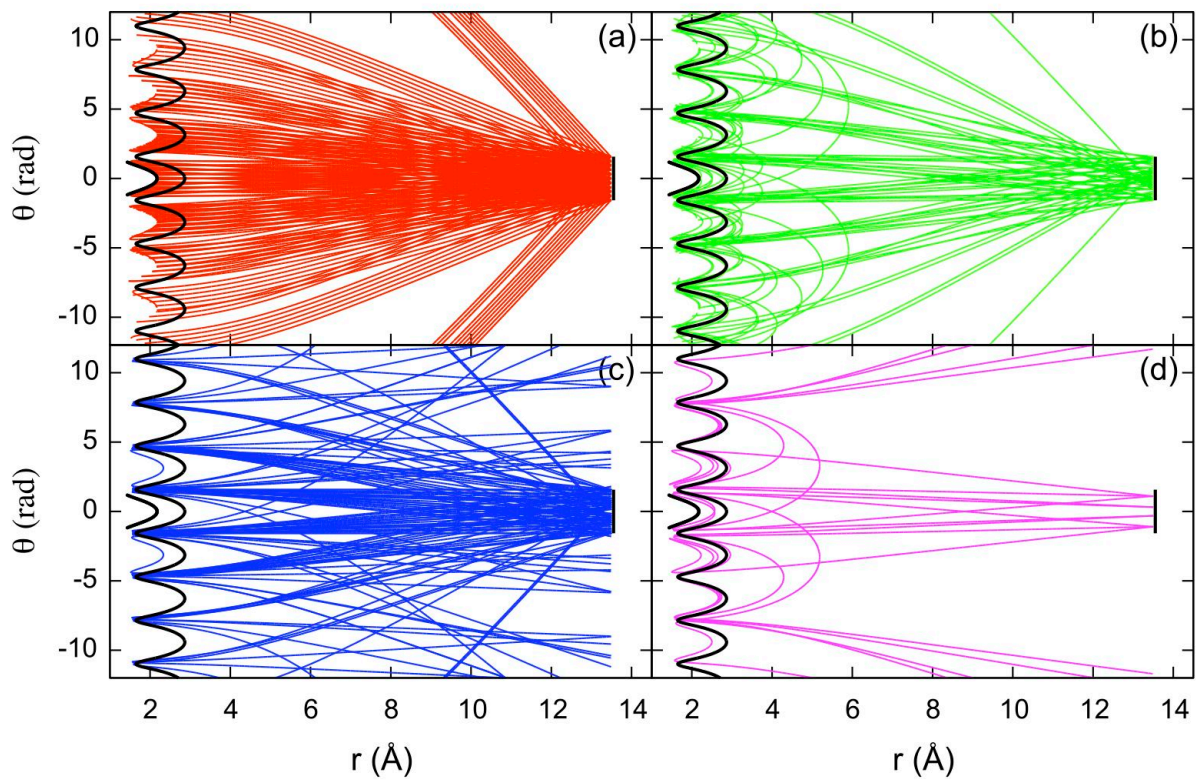


FIG. 4: The four different types of trajectories for the case  $\alpha = 4$ . The thick black curves correspond to the TTS-PO, FR1 PO and OTS PO, respectively. (a) Direct reactive trajectories (red). (b) Roaming reactive trajectories (green). (c) Direct non reactive trajectories (blue). (d) Roaming non reactive trajectories (magenta).

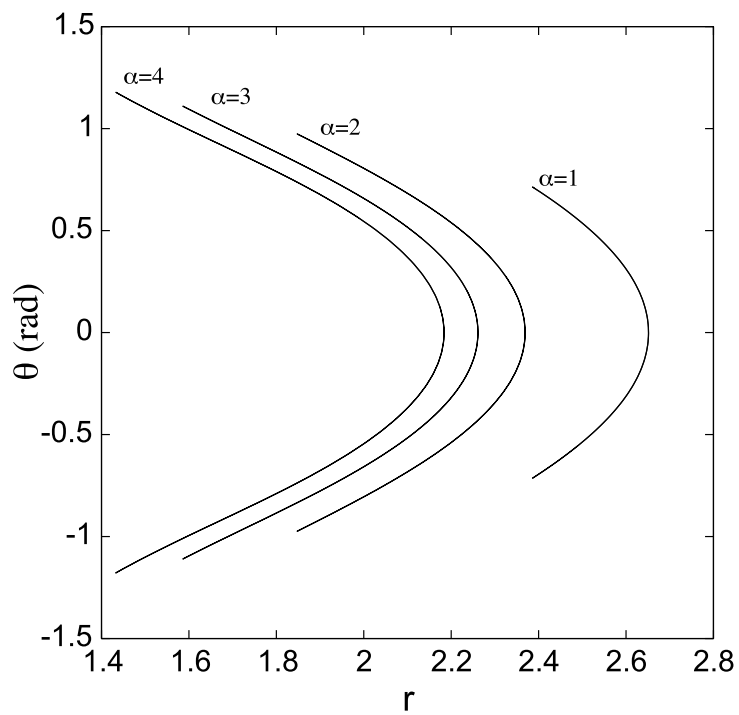


FIG. 5: Evolution of the TTS-PO with parameter  $\alpha$ . Constant energy of  $0.5 \text{ kcal.mol}^{-1}$

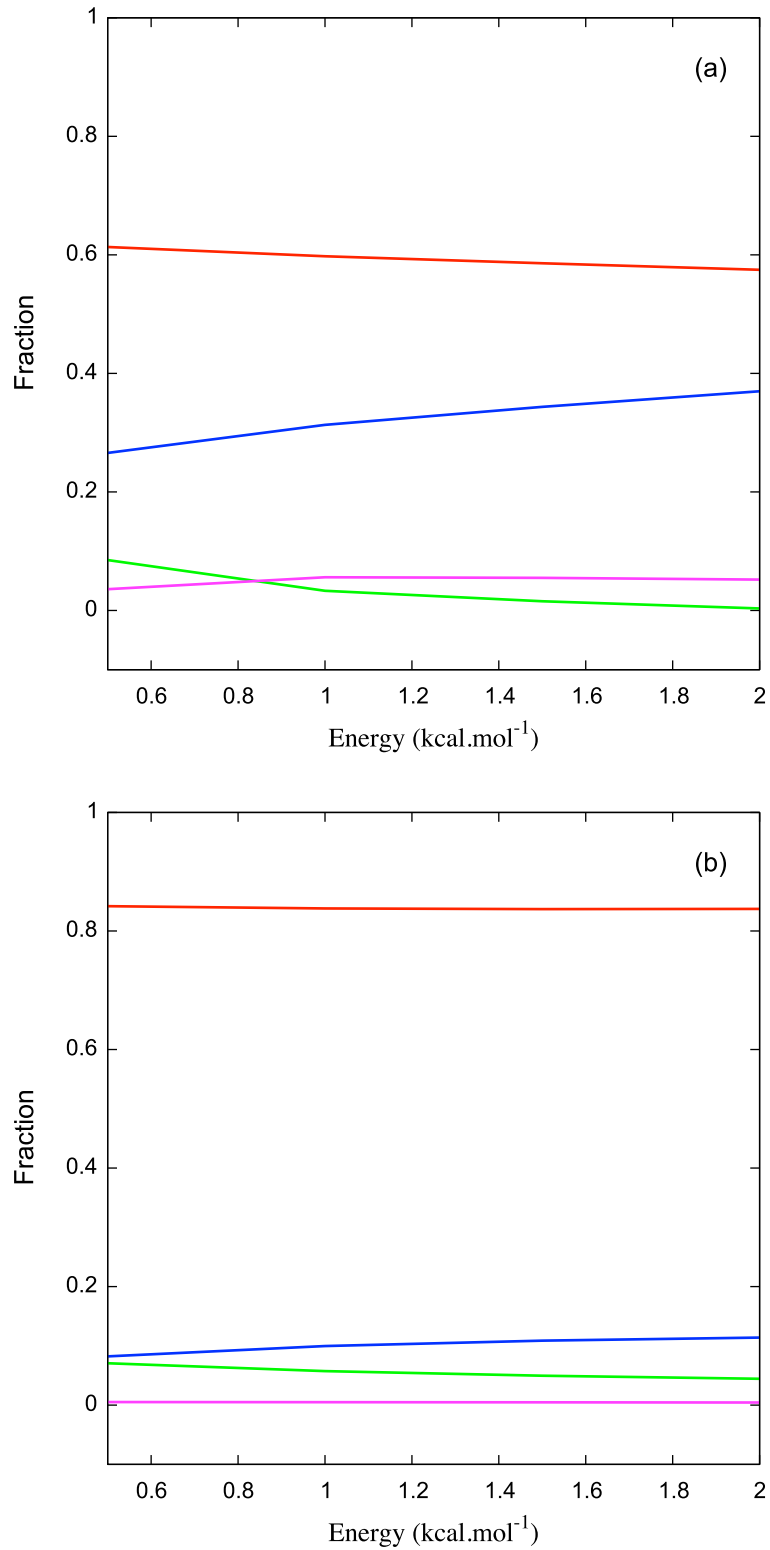


FIG. 6: (color online) Fractions of different types of trajectories versus energy. Red line is the fraction of direct reactive trajectories, green for roaming reactive trajectories, blue for direct non reactive and magenta for roaming non reactive trajectories. (a)  $\alpha = 1$ , (b)  $\alpha = 4$ .

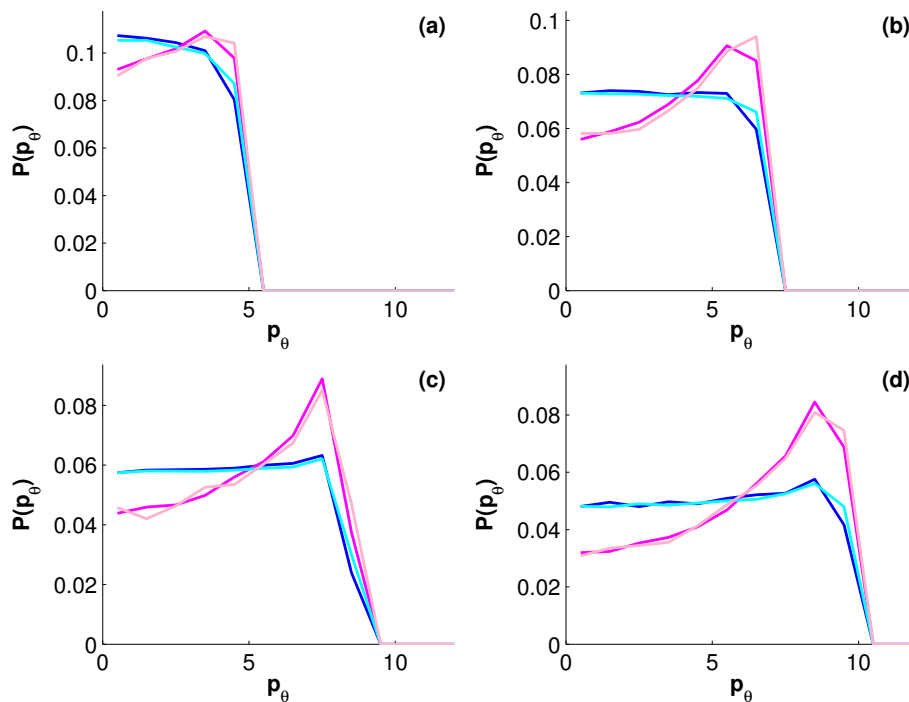


FIG. 7: Initial and final normalised  $p_\theta$  distributions for  $\alpha = 1$ . Blue and magenta curves represent initial distributions for direct non reactive and roaming non reactive trajectories, respectively, and cyan and pink curves represent the final distributions for direct non reactive and roaming non reactive trajectories, respectively. (a) Energy  $E=0.5$  kcal.mol $^{-1}$ . (b)  $E=1.0$  kcal.mol $^{-1}$ . (c)  $E=1.5$  kcal.mol $^{-1}$ . (d)  $E=2.0$  kcal.mol $^{-1}$ .

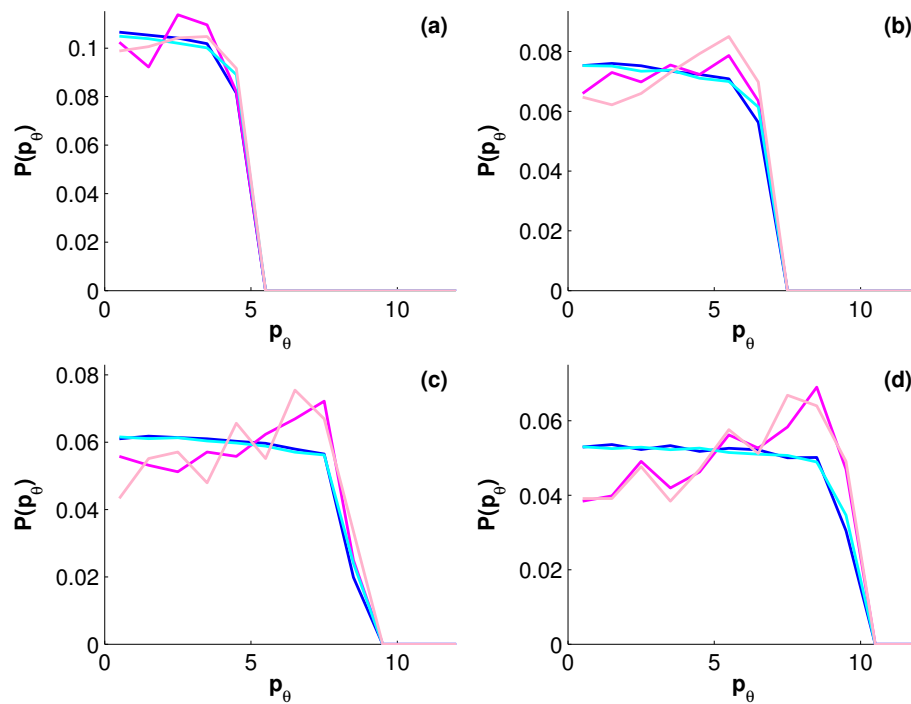


FIG. 8: Initial and final normalised  $p_\theta$  distributions for  $\alpha = 4$ . Blue and magenta curves represent initial distributions for direct non reactive and roaming non reactive trajectories, respectively, and cyan and pink curves represent the final distributions for direct non reactive and roaming non reactive trajectories, respectively. (a) Energy  $E=0.5$  kcal.mol $^{-1}$ . (b)  $E=1.0$  kcal.mol $^{-1}$ . (c)  $E=1.5$  kcal.mol $^{-1}$ . (d)  $E=2.0$  kcal.mol $^{-1}$ .

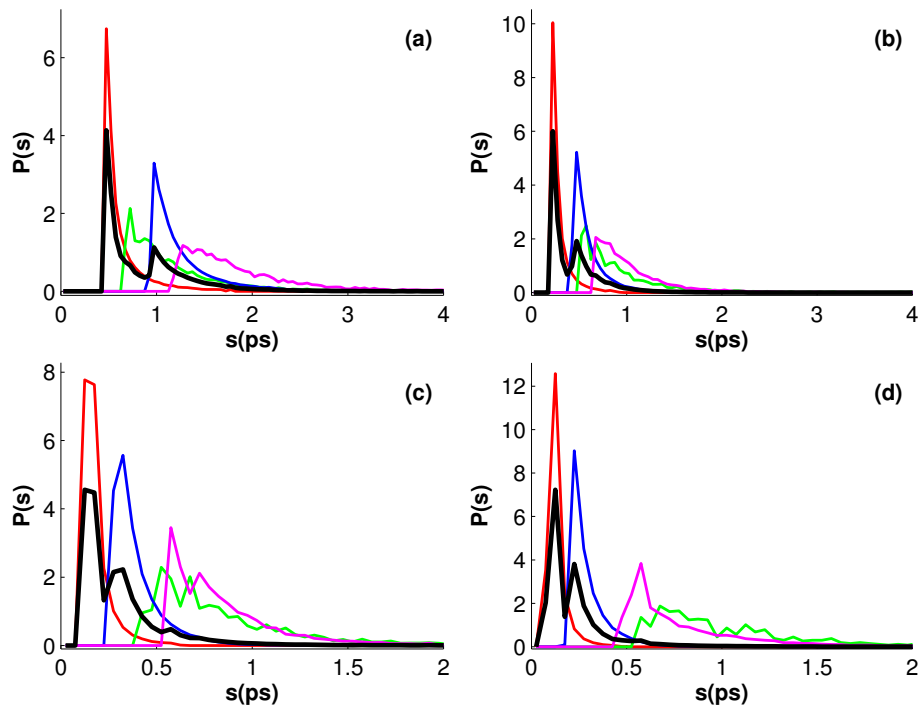


FIG. 9: Gap time distributions for  $\alpha = 1$ . In each panel, red line denotes the normalised gap time distribution of direct reactive trajectories, green for roaming reactive trajectories, blue for direct non reactive and magenta for roaming non reactive trajectories. The thick black curve denotes the normalised gap time distribution for all trajectories. (a) Energy  $E=0.5$  kcal.mol $^{-1}$ . (b)  $E=1.0$  kcal.mol $^{-1}$ . (c)  $E=1.5$  kcal.mol $^{-1}$ . (d)  $E=2.0$  kcal.mol $^{-1}$ .



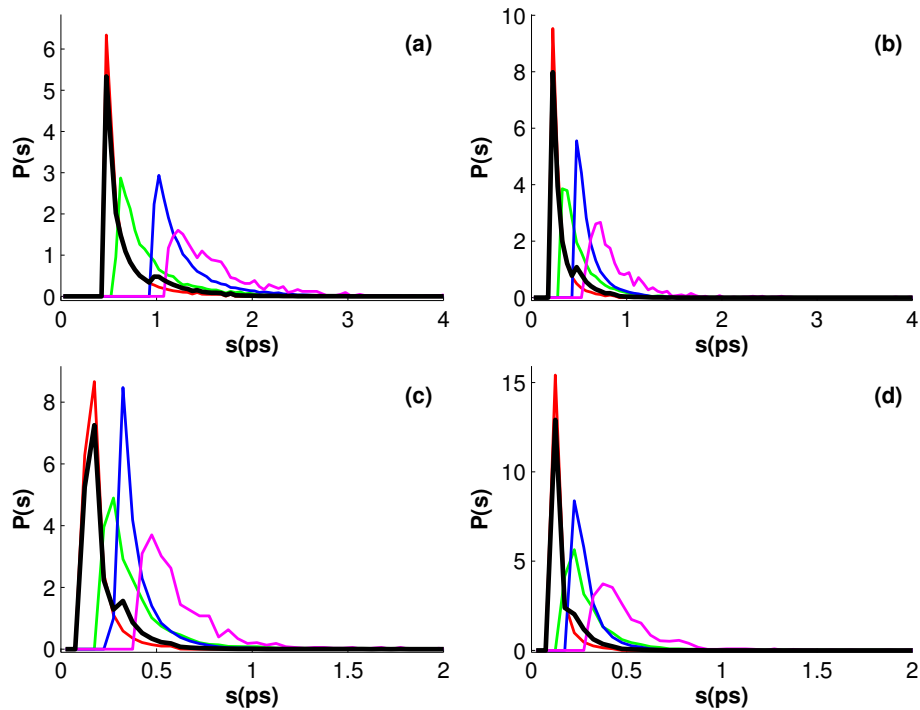


FIG. 10: Gap time distributions for  $\alpha = 4$ . In each panel, red line denotes the normalised gap time distribution of direct reactive trajectories, green that for roaming reactive trajectories, blue for direct non reactive trajectories and magenta for roaming non reactive trajectories. The thick black curve denote the normalised gap time distribution for all trajectories. (a) Energy  $E=0.5$  kcal.mol $^{-1}$ . (b)  $E=1.0$  kcal.mol $^{-1}$ . (c)  $E=1.5$  kcal.mol $^{-1}$ . (d)  $E=2.0$  kcal.mol $^{-1}$ .

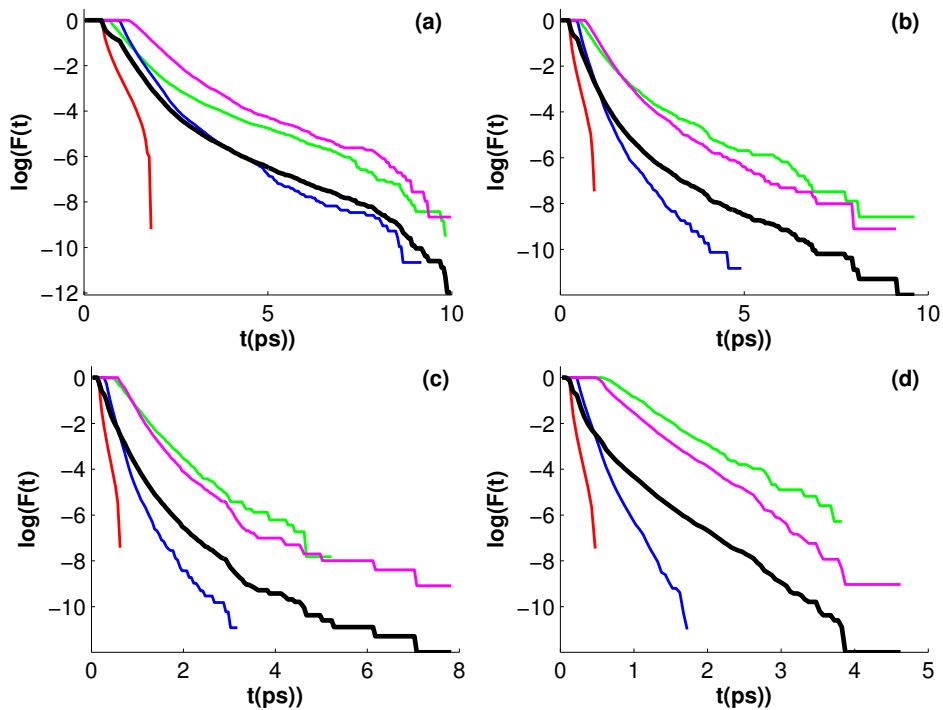


FIG. 11: The logarithm of the lifetime distributions for  $\alpha = 1$ . In each panel, red line denotes the normalised logarithm of the lifetime distribution of direct reactive trajectories, green for roaming reactive trajectories, blue for direct non reactive and magenta for roaming non reactive trajectories. The thick black curve denotes the normalised logarithm of the lifetime for all trajectories. (a) Energy  $E=0.5$  kcal.mol $^{-1}$ . (b)  $E=1.0$  kcal.mol $^{-1}$ . (c)  $E=1.5$  kcal.mol $^{-1}$ . (d)  $E=2.0$  kcal.mol $^{-1}$ .

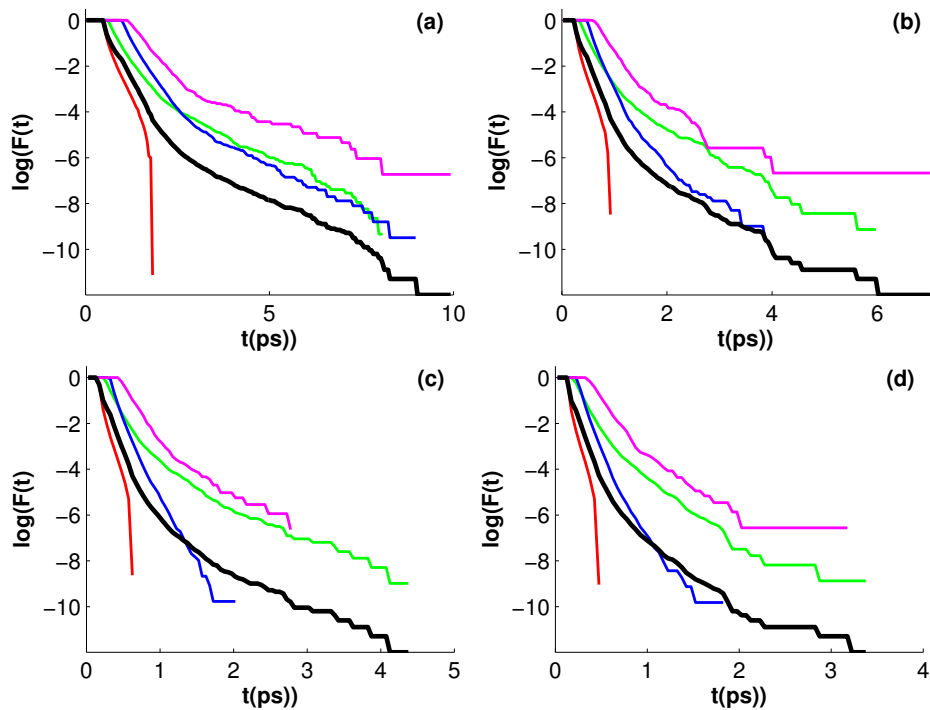


FIG. 12: The logarithm of the lifetime distributions for  $\alpha = 4$ . In each panel, red line denotes the normalised logarithm of the lifetime distribution of direct reactive trajectories, green for roaming reactive trajectories, blue for direct non reactive and magenta for roaming non reactive trajectories. The thick black curve denotes the normalised logarithm of the lifetime for all trajectories. (a) Energy  $E=0.5$  kcal.mol $^{-1}$ . (b)  $E=1.0$  kcal.mol $^{-1}$ . (c)  $E=1.5$  kcal.mol $^{-1}$ . (d)  $E=2.0$  kcal.mol $^{-1}$ .

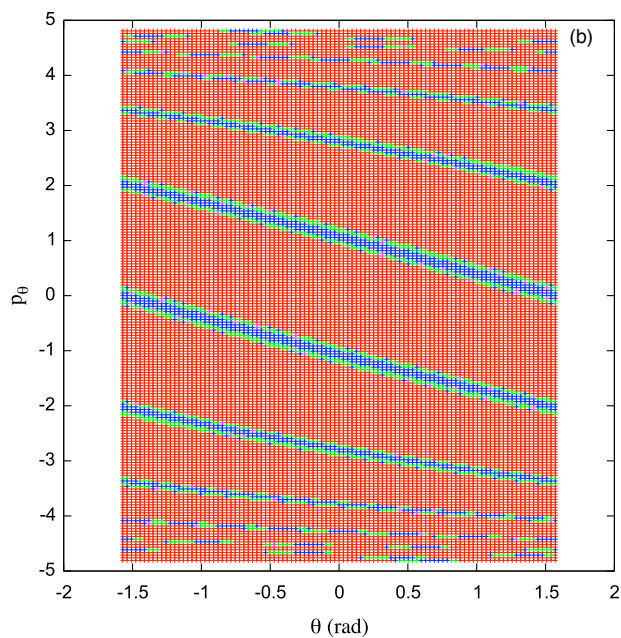
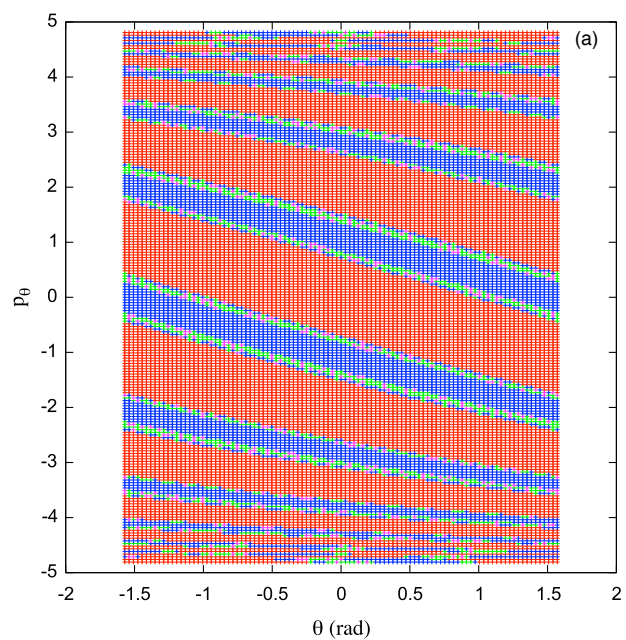


FIG. 13: Distribution of the different types of trajectories on the OTS. (a)  $\alpha = 1$ , energy  $E=0.5$  kcal.mol<sup>-1</sup>. (b)  $\alpha = 4$ , energy  $E=0.5$  kcal.mol<sup>-1</sup>

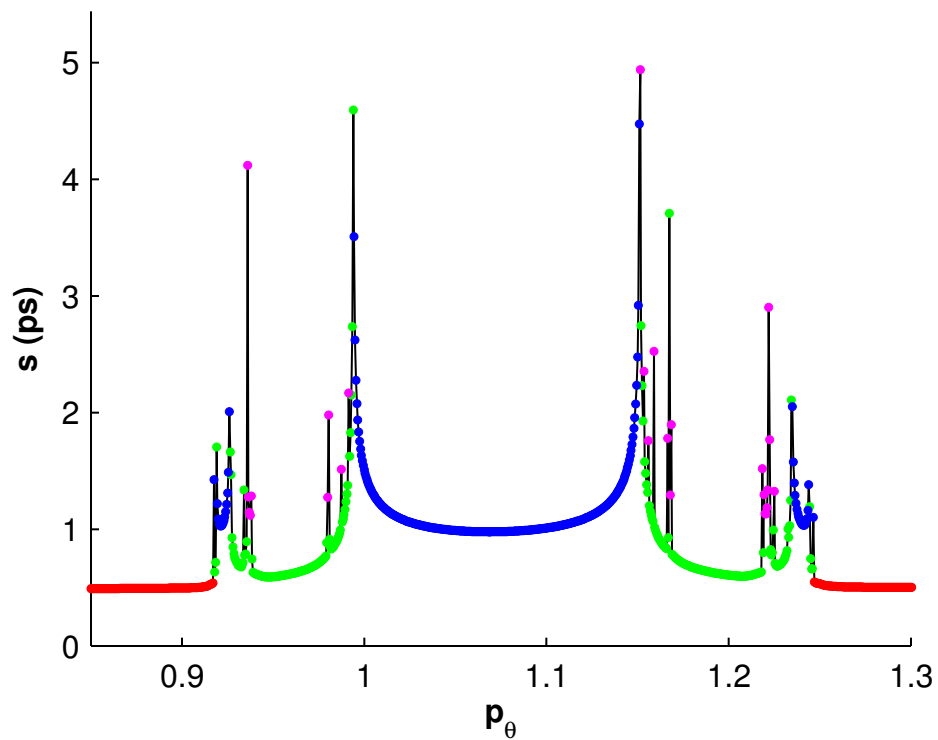


FIG. 14: The fractal nature of the boundaries between different types of trajectories on the DS. Initial points are selected along the line  $\theta = 0$  on the OTS, with  $\alpha = 4$  and energy  $E=0.5 \text{ kcal.mol}^{-1}$ . The vertical axis shows the gap time and sampling points are assigned a colour to mark their type. Red: direct reactive trajectories, green: roaming reactive trajectories, blue: direct non reactive and magenta: roaming non reactive trajectories.